

Discrete Modeling for Natural Objects¹

J. L. Mallet²

This paper presents a discrete technique specially designed for modeling the geometry and the properties of natural objects as those encountered in biology and geology. Contrary to classical Computer-Aided Design methods based on continuous (polynomial) functions, the proposed approach is based on a discretization of the objects close to the finite-element techniques used for solving differential equations. Each object is modeled as a set of interconnected nodes holding the geometry and the physical properties of the objects and the Discrete Smooth Interpolation method is used for fitting the geometry and the properties to complex data. Data are turned into linear constraints and some constraints related to typical information encountered in geology are presented.

KEY WORDS: DSI, interpolation, geometrical modeling.

INTRODUCTION

In this introduction, we would like to emphasize the need for a new breed of Computer-Aided Design (CAD) specially dedicated to the modeling of natural objects such as those encountered in biology and geology. In a nutshell, we could say that a user of a classical CAD software is creating nice curves, surfaces, and volumes without any constraint whereas a user of a CAD software dedicated to the modeling of natural objects has to respect constraints induced by the observed data. All of these classical CAD software are based parametric methods such as those introduced by Bezier (1974) in the early 1970s.

The goal of the mathematicians who designed these methods (Bezier, 1974; de Boor, 1978; Farin, 1988, . . .) was simply to propose tools for modeling interactively nice curves and surfaces and not to respect complex data as those that we can encounter in geology. For example, if we consider the geological horizon (= surface) represented in Figure 1, we can say that the data available are complex for the following reasons:

¹Received 15 December 1995; revised 19 July 1996.

²Computer Science Department (CRIN, CRPG), Ecole Nationale Supérieure de Géologie, Rue du Doyen Marcel Roubault-B.P.40, 54501 Vandœuvre-les-Nancy, France; e-mail: mallet@ensg.u-nancy.fr

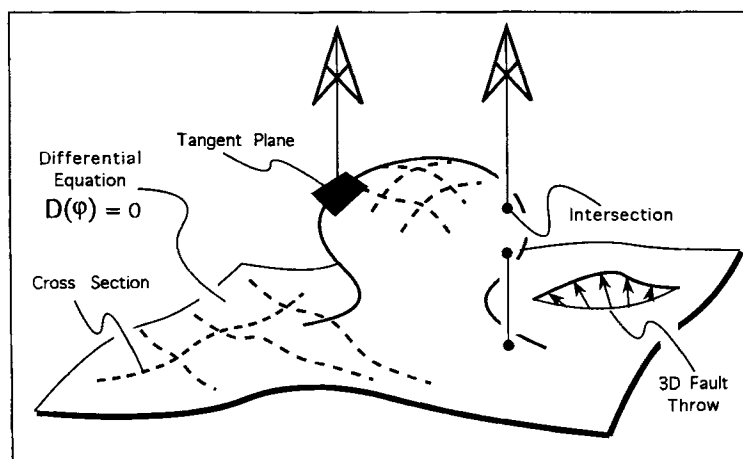


Figure 1. Example of complex data to take into account when modeling geological horizon.

- The data are heterogeneous because it is necessary to account simultaneously for:
 - the locations of the intersections of the well curves with the surface to be modeled,
 - the slope of the tangent plane to the surface when this slope has been measured at the intersections of the wells with the surface,
 - seismic data corresponding to cross sections of the surface;
 - structural information consisting of 3D fault throw vectors;
 - mechanical information specifying that the surface should respect a given differential equation; and
 - physical properties (seismic velocities, reflectivities, . . .) attached to the surface and observed directly or indirectly at some locations.
- The data are more or less reliable; for example, well data are more reliable than seismic data which in turn are more reliable than structural data.
- The data are distributed irregularly and generally are clustered strongly on lines and surfaces. In practice, this clustering generates numerical instabilities in most of the numerical methods used for interpolating the data.

Another major drawback with classical CAD methods is that they have been designed for modeling the geometry of objects and not to take care of the physical properties attached to these objects. In geology, there is a need for modeling simultaneously the geometry and the properties and there are many

situations where the geometry and the properties are linked: for example, the seismic velocity in a layer depends on the position relative to the hanging and foot walls of the layer whose geometry depends in turn on the seismic velocity.

Mathematical methods used in classical CAD have not been designed for addressing such complex data and it is too optimistic to think that these methods could be adapted in order to account simultaneously for all of the data available while respecting their complexity (Mallet, 1992a). In fact, these methods have been designed initially for the needs of the car industry (Bezier, 1974) and it is necessary to look for a specific class of mathematical modeling methods specially designed for the needs of the geosciences.

The success of polynomial models used in classical CAD (Mortenson, 1985) comes from the fact that polynomials generate aesthetic curves and surfaces and this is of paramount importance in the car industry (Bezier, 1974). However, in the geosciences, our primary concern is more to respect the constraints induced by the data than to produce nice-looking objects. It generally is admitted that discretized problems are simpler to solve than problems based on continuous representations and this is why, in this paper, we propose to abandon the polynomial models used in classical CAD in favor of a discrete approach close to the “finite elements” technique used for solving differential equations.

Despite the fact that they are less well known than parametric methods, discrete modeling methods have been presented in various particular forms and implementations for about 70 years. Examples include: Whittaker (1923), Horton (1923), Bergthorsson and Doos (1995), Weaver (1964), Arthur (1965), Harder and Desmarais (1972), Briggs (1974), Akima (1978), Sibson (1981), Mallet (1992b), and Overveld (1995). The goal of this paper is to propose a generic formulation of discrete modeling which generalizes most of these methods.

The approach presented in this paper was designed specially for modeling natural objects and is potentially able to account for any series of (linear) constraints corresponding to the influence of the data on the model. Each of these constraints can be weighted by a “certainty factor” used for specifying its importance relative to the other constraints. This is particularly interesting in the geosciences where, because of sampling errors, it may happen that some constraints become contradictory; for example, if the projection of two seismic cross sections in the (x, y) horizontal plane are crossing at some point $P(x, y)$, it is almost sure that these two seismic cross sections do not actually cross in the (x, y, z) 3D-space (see Fig. 1) and it is important to be able to weight each of them with a given certainty factor proportional to the quality of the data.

DISCRETE MODELING

In this section, a general formulation of the notion of a discrete model is presented which can be used for approximating complex objects such as those encountered, for example, in the geosciences.

Discrete Topological Model $\mathcal{G}(\Omega, N)$

As shown in Figures 2 and 3, the main idea in a discrete model is that the topology of any object can be approximated by a graph $\mathcal{G}(\Omega, N)$ where:

- Ω is the set of all the nodes of the graph, each of these nodes being identified with its rank order:

$$\Omega = \{1, 2, \dots, \alpha, \dots, M\}$$

- N is an application from Ω into a subset of Ω such that

$$\{\beta \in N(\alpha)\} \Leftrightarrow \{\beta \text{ can be reached in at most } s(\alpha) \text{ steps from } \alpha\}$$
- where $s(\alpha) > 0$ is a given function of the node α . In practice, in order to minimize the complexity of the model, we suggest selecting $s(\alpha) = 1$ but, from a mathematical point of view, this is absolutely not mandatory. It is assumed also that the graph $\mathcal{G}(\Omega, N)$ is symmetric and this

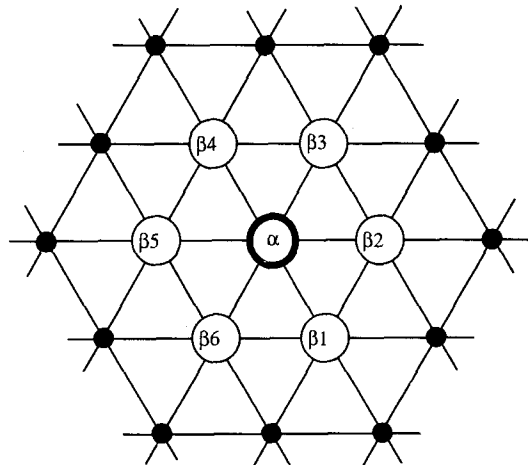


Figure 2. Neighborhood $N(\alpha)$ of node α is composed of α plus all nodes of its orbit $\Lambda(\alpha) = \{\beta_1, \beta_2, \dots\}$. This figure corresponds to special situation where $N(\alpha)$ is defined as set of nodes which can be reached in at most $s(\alpha) = 1$ step from α .

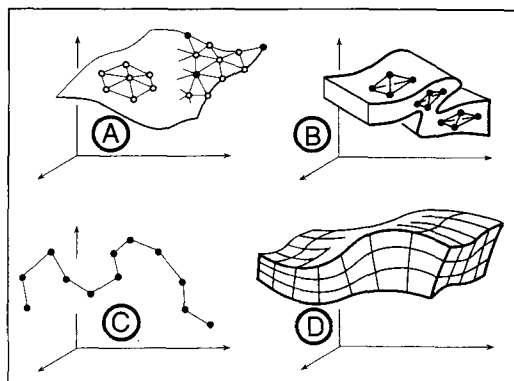


Figure 3. Examples of objects approximated by discrete model: A, triangulated geological surface; B, tetrahedralized layer; C, polygonal curve corresponding to cross section of geological surfaces; and D, curvilinear grid filling layer.

implies that $N(\cdot)$ is such that:

$$\beta \in N(\alpha) \Leftrightarrow \alpha \in N(\beta)$$

The subset $N(\alpha)$ is termed ‘‘neighborhood’’ of α and it must be noted that $N(\alpha)$ contains the node α and all its surrounding nodes (see Fig. 2):

$$N(\alpha) = \{\alpha, \beta_1, \beta_2, \dots\}$$

From a mathematical point of view (Bass, 1971), it can be said that $N(\cdot)$ defines a discrete topology on Ω in this sense that:

$$\beta \in N(\alpha) \Leftrightarrow \alpha \in N(\beta) \Leftrightarrow \alpha \text{ is ‘‘close’’ to } \beta$$

As suggested in Figure 2, the ‘‘orbit’’ $\Lambda(\alpha)$ of a node α is defined as the set of nodes $\{\beta_1, \beta_2, \dots\}$ different from α and belonging to $N(\alpha)$:

$$\Lambda(\alpha) = N(\alpha) - \{\alpha\}$$

Examples of Discrete Topological Models

Potentially, the notion of Discrete Topological Model presented in the previous section can be used for modeling the topology of any geological object. For example and as suggested in Figure 3, it is possible to model:

- a geological horizon or a fault (surface) as a set of adjacent triangles (Fig. 3A and 4A).

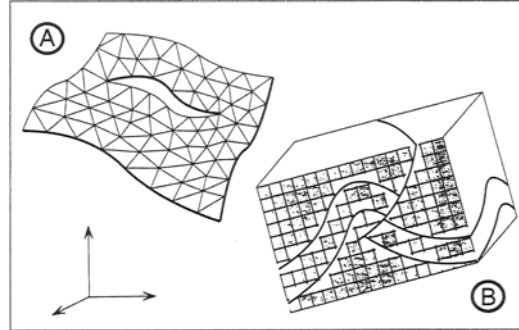


Figure 4. Discontinuities are introduced in the graph $\mathcal{G}(\Omega, N)$ by removing some edges from network A and B. In grid B, all edges intersected by geological surfaces (horizons and faults) have been removed.

- a geological body (solid) as a set of adjacent tetrahedra (Fig. 3B).
- a geological cross section (curve) as a set of adjacent segments (Fig. 3C).
- a geological layer (solid) as a regular curvilinear or rectilinear grid (Figs. 3D and 4B).

In these models, the vertices of the triangles, tetrahedra, and segments correspond to the nodes of $\mathcal{G}(\Omega, N)$ whereas the edges define the topology. The introduction of a discontinuity between two adjacent nodes α and β is straightforward and, as suggested in Figure 4, this can be achieved simply by removing the edge (α, β) from the network.

Notion of Discrete Model $\mathfrak{M}(\Omega, N, \varphi, \mathcal{C})$

The discrete topological model $\mathcal{G}(\Omega, N)$ introduced in the previous sections does not take care of the properties of the objects. Such properties are modeled as a series φ of numerical functions, termed components of φ , defined on the set of nodes Ω of $\mathcal{G}(\Omega, N)$:

$$\varphi(\alpha) = \{\varphi^x(\alpha), \varphi^y(\alpha), \varphi^z(\alpha), \dots, \varphi^v(\alpha), \dots\} \quad \forall \alpha \in \Omega$$

In practice, the three first components $\{\varphi^x(\alpha), \varphi^y(\alpha), \varphi^z(\alpha)\}$ correspond to the location of the node $\alpha \in \Omega$ in the 3D space whereas the other functions correspond to physical properties.

By definition, the notion of discrete model $\mathfrak{M}(\Omega, N, \varphi, \mathcal{C})$ consists of a triplet composed of $\mathcal{G}(\Omega, N)$, the functions φ , and a set of constraints $\mathcal{C} = \{C_1,$

$C_2, \dots\}$:

$$\mathfrak{N}(\Omega, N, \varphi, \mathcal{C}) = \{\mathfrak{S}(\Omega, N), \varphi, \mathcal{C}\}$$

Each constraint $C_i \in \mathcal{C}$ is assumed to be linear and to have the following general form where $A_i^\nu(\alpha)$ and b_i are given coefficients:

$$\{C_i \text{ satisfied}\} \Leftrightarrow \sum_{\alpha \in \Omega} \sum_{\nu} A_i^\nu(\alpha) \cdot \varphi^\nu(\alpha) = b_i$$

In practice, the coefficients $A_i^\nu(\alpha)$ and b_i are determined in function of the available data, for example:

- If we want $\varphi^\eta(\alpha_0)$ to be equal to a given value φ_0^η at node α_0 , then this data easily can be turned into a constraint C_i such that:

$$\left| \begin{array}{l} A_i^\nu(\alpha) = \begin{cases} 1 & \text{if } \alpha = \alpha_0 \text{ \& } \nu = \eta \\ 0 & \text{otherwise} \end{cases} \\ b_i = \varphi_0^\nu \end{array} \right.$$

On Figure 1, this constraint can be used for specifying that the coordinates $(\varphi^x(\alpha_0), \varphi^y(\alpha_0), \varphi^z(\alpha_0))$ of a node α_0 of the surface should be equal to the coordinates of the intersection of the well with the surface.

- If we want the gradient of φ^η to be equal to a given value of $\Delta^\eta(\alpha_0, \alpha_1)$ between two nodes (α_0, α_1) , then this implies that

$$\varphi^\eta(\alpha_0) - \varphi^\eta(\alpha_1) = \Delta^\eta(\alpha_0, \alpha_1)$$

and this information can be easily turned into a constraint C_i such that:

$$\left| \begin{array}{l} A_i^\nu(\alpha) = \begin{cases} 1 & \text{if } \alpha = \alpha_0 \text{ \& } \nu = \eta \\ -1 & \text{if } \alpha = \alpha_1 \text{ \& } \nu = \eta \\ 0 & \text{otherwise} \end{cases} \\ b_i = \Delta^\eta(\alpha_0, \alpha_1) \end{array} \right.$$

On Figure 1 and 4A, this constraint can be used for specifying that the coordinates $(\varphi^x(\alpha_0), \varphi^y(\alpha_0), \varphi^z(\alpha_0))$ and $(\varphi^x(\alpha_1), \varphi^y(\alpha_1), \varphi^z(\alpha_1))$ of two nodes located on both sides of a fault should be equal to a given throw vector $(\Delta^x(\alpha_0, \alpha_1), \Delta^y(\alpha_0, \alpha_1), \Delta^z(\alpha_0, \alpha_1))$.

- If we want the point $\{\varphi^x(\alpha_0), \varphi^y(\alpha_0), \varphi^z(\alpha_0)\}$ be located on a given plane $\mathcal{P}(p, n)$ containing the point $p = (p^x, p^y, p^z)$ and orthogonal to the vector $n = (n^x, n^y, n^z)$, then we should have

$$\varphi^x(\alpha_0) \cdot n^x + \varphi^y(\alpha_0) \cdot n^y + \varphi^z(\alpha_0) \cdot n^z = p^x \cdot n^x + p^y \cdot n^y + p^z \cdot n^z$$

and this relationship can be turned easily into a constraint C_i such that:

$$A_i^v(\alpha) = \begin{cases} n^x & \text{if } \alpha = \alpha_0 \text{ \& } v = x \\ n^y & \text{if } \alpha = \alpha_0 \text{ \& } v = y \\ n^z & \text{if } \alpha = \alpha_0 \text{ \& } v = z \\ 0 & \text{otherwise} \end{cases}$$

$$b_i = p^x \cdot n^x + p^y \cdot n^y + p^z \cdot n^z$$

It is important to notice that, contrary to the two previous constraints as presented, this constraint is a ‘‘cross’’ constraint merging several components of φ .

On Figure 1, this constraint can be used for specifying that a node α_0 should be located in a given tangent plane.

- If φ^v is the pressure of water (or oil) in a given layer, then φ^v has to respect the diffusion equation. Such an equation can be discretized with a finite difference or finite element method (Aziz and Settari, 1979) based on $\mathcal{G}(\Omega, N)$ in such a way that this equation reduces to a linear constraint C_i

$$\sum_{\alpha \in \Omega} \sum_v A_i^v(\alpha) \cdot \varphi^v(\alpha) = b_i$$

- where the coefficients $A_i^v(\alpha)$ and b_i depend only on the geometry (φ^x , φ^y , φ^z) and the permeability φ^p of the model.

As you can see, the formulation that we have adopted is general and, for any elementary data, we have to look for a linear operator translating the influence of this data on φ . Most of the time, the constraints are actually linear relative to the values $\{\varphi(\alpha): \alpha \in \Omega\}$ but there are some situations where we are faced with nonlinear constraints; for example, if we want that a given component φ^v of φ have a given Cumulative Distribution Function $F^v(z)$, then it can be verified that the corresponding constraint is not linear. When a constraint is not linear, it is possible to use the Taylor approximation for linearizing it (Gill, Murray, and Wright, 1981) relative to the values $\{\varphi(\alpha): \alpha \in \Omega\}$ in the neighborhood of a given initial solution $\varphi_{[0]}$.

INTERPOLATION

In this section, the Discrete Smooth Interpolation Method (abbreviated DSI) is presented which has been designed specifically for interpolating the function φ of a discrete model $\mathfrak{M}(\Omega, N, \varphi, \mathcal{C})$ while respecting all the constraints $C_i \in \mathcal{C}$. Contrary to the general presentations in the literature (Mallet, 1989b, 1992b;

Overveld, 1995) that focus on mathematical aspects of this method, here we are concerned mainly by showing that this method in fact is simple and can be easily understood.

Introduction

As suggested in Figure 5, let us consider an ordinary function φ defined on the segment $\tilde{\Omega} = [1, M]$ and let Ω be the set of nodes corresponding to the regular sampling of $\tilde{\Omega}$ with a step equal to 1:

$$\Omega = \{1, 2, \dots, M\}$$

In Figure 5, the nodes $\alpha \in \Omega$ correspond to the white points whereas black points correspond to some given data points $\{\ell, \varphi(\ell): \ell \in \Omega\}$ that we would like to interpolate. For that purpose, a classic method (de Boor, 1978; Farin, 1988) consists of looking for a spline function φ minimizing the “global roughness” $\tilde{R}(\varphi)$ such that:

$$\left\{ \begin{array}{l} \tilde{R}(\varphi) = \int_{\Omega} \mu(x) \cdot \tilde{R}(\varphi|x) \cdot dx \\ \text{with : } \tilde{R}(\varphi|x) = \left| \frac{d^2\varphi}{dx^2} \right|^2 \end{array} \right.$$

In this expression, $\mu(x) > 0$ is a given local “stiffness” coefficient (that we can take constant equal to 1 for example) while $\tilde{R}(\varphi|x)$ can be interpreted as a

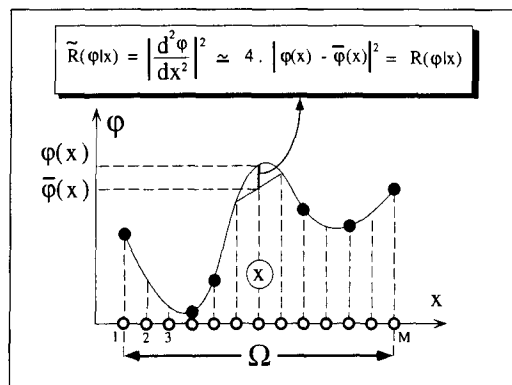


Figure 5. Local roughness $\tilde{R}(\varphi|x)$ of spline curve $\varphi(x)$ at node x is proportional to square of length of segment $|\varphi(x) - \bar{\varphi}(x)|$.

measure of the “local roughness” of φ at point $x \in \Omega$. If we let

$$\bar{\varphi}(x) = \frac{\varphi(x-1) + \varphi(x+1)}{2}$$

then, as suggested in Figure 5, we can verify that a finite difference approximation of $d^2\varphi/dx^2$ is such that:

$$\frac{d^2\varphi}{dx^2} \approx 2 \cdot \{\bar{\varphi}(x) - \varphi(x)\} = \{1 \cdot \varphi(x-1) + 1 \cdot \varphi(x+1)\} - 2 \cdot \varphi(x)$$

If we neglect the side effects which occur at node $\alpha = 1$ and $\alpha = M$, then, for any $k \in \Omega$, we can write:

$$\left| \begin{array}{l} \tilde{R}(\varphi|k) \approx \left| \sum_{k \in N(\alpha)} v^\alpha(k) \cdot \varphi(\alpha) \right|^2 \\ \text{with: } \begin{cases} v^\alpha(k) = 1 & \text{if } \alpha \in \Lambda(k) \\ v^k(k) = -2 & \text{otherwise} \end{cases} \end{array} \right.$$

If we let

$$\left| \begin{array}{l} R(\varphi) = \sum_{\alpha \in \Omega} \mu(k) \cdot R(\varphi|k) \\ \text{with: } R(\varphi|k) = \left| \sum_{k \in N(\alpha)} v^\alpha(k) \cdot \varphi(\alpha) \right|^2 \end{array} \right.$$

then it can be said that $R(\varphi)$ is an approximation of the global roughness $\tilde{R}(\varphi)$:

$$R(\varphi) \approx \tilde{R}(\varphi)$$

Thus it is concluded that it is approximately equivalent to minimize $\tilde{R}(\varphi)$ or $R(\varphi)$ and this remark is at the origin of the Discrete Smooth Interpolation method (Mallet, 1989b, 1992b) presented in the next sections.

Discrete Smooth Interpolation

Now consider a discrete model $\mathfrak{M}(\Omega, N, \varphi, \mathbb{C})$ where φ is assumed to have only one component so that we will make no distinction in this paragraph between φ and its unique component. Let L and I be two complementary subsets of Ω such that:

$$\left| \begin{array}{l} L = \text{set of nodes } \ell \in \Omega \text{ where } \varphi(\ell) \text{ is known} \\ I = \text{set of nodes } i \in \Omega \text{ where } \varphi(i) \text{ is unknown} \\ = \Omega - L \end{array} \right.$$

The set L is termed set of “control nodes” and the values $\{\varphi(i): i \in I\}$ should be computed in such a way that the resulting function φ be “as smooth as possible” on $\mathcal{G}(\Omega, N)$ whereas respecting strictly the “control values” $\{\varphi(\ell): \ell \in L\}$ and respecting “as much as possible” each of the constraints $C_i \in \mathcal{C}$. For that purpose, it proposed to measure the local roughness $R(\varphi|k)$ of φ in the neighborhood of each node $k \in \Omega$ and the degree of violation $\rho(\varphi|C_i)$ of each constraint $C_i \in \mathcal{C}$ by φ as follows:

$$R(\varphi|k) = \left| \sum_{\alpha \in \Lambda(k)} v^\alpha(k) \cdot \varphi(\alpha) \right|^2$$

$$\rho(\varphi|C_i) = \left| \sum_{\alpha \in \Omega} A_i(\alpha) \cdot \varphi(\alpha) - b_i \right|^2$$

In the definition of the local roughness $R(\varphi|k)$ above, the $\{v^\alpha(k)\}$ are given coefficients and the Discrete Smooth Interpolation method (DSI), proposes to look for a function φ minimizing the following “generalized roughness” criterion $R^*(\varphi)$:

$$R^*(\varphi) = \sum_{k \in \Omega} \mu(k) \cdot R(\varphi|k) + \sum_i \bar{\omega}_i \cdot \rho(\varphi|C_i)$$

In this criterion, $\mu(k) > 0$ is a given positive “stiffness” function modulating the importance of the local roughness $R(\varphi|k)$ at node k while the coefficients $\{\bar{\omega}_i\}$ are positive “certainty factors” weighting the relative importance of each of the constraints.

It can be shown (Mallet, 1992b) that the solution φ minimizing $R^*(\varphi)$ exists and is unique if the following general conditions are respected:

$$\left\{ \begin{array}{l} 1) \quad L \text{ is not empty} \\ 2) \quad \left\{ \begin{array}{l} v^\alpha(k) > 0 \quad \forall \alpha \in \Lambda(k) \\ v^k(k) = - \sum_{\alpha \in \Lambda(k)} v^\alpha(k) \end{array} \right. \\ 3) \quad \left\{ \begin{array}{l} \mu(k) > 0 \quad \forall k \in \Omega \\ \bar{\omega}_i > 0 \quad \forall i \end{array} \right. \end{array} \right.$$

It is important to notice that these conditions are sufficient for ensuring the existence and the uniqueness of the solution φ but they are not necessary. By the way, the conditions (2) are satisfied by the coefficients $\{v^\alpha(k)\}$ proposed in the introduction in connection with the spline interpolation method.

Remarks

- There is a wide variety of possible selections for the coefficients $\{v^\alpha(k)\}$ respecting the conditions (2) presented in the previous paragraph. As you can imagine, the solution φ depends on these selections and, from this point of view, the DSI method seems as a “generic” method able to produce different styles of solutions.

Mallet (1992a, 1992b) describes several possible selections for the coefficients $\{v^\alpha(k)\}$ and the most simple selection correspond to the so-called “*harmonic weightings*” producing solutions “*a la spline*” and such that:

$$v^\alpha(k) = \begin{cases} -|\Lambda(k)| & \text{if } \alpha = k \\ 1 & \text{if } \alpha \in \Lambda(k) \end{cases}$$

In this expression, $|\Lambda(k)|$ represents the number of elements in the orbit $\Lambda(k)$ and, in the situation where $\mathcal{G}(\Omega, N)$ is a polygonal curve, the coefficients $\{v^\alpha(k)\}$ are exactly the ones we encountered in the introduction.

- It also is important to mention that the coefficients $\{v^\alpha(k)\}$ can be used for modeling nonconstant anisotropies. In this instance, the magnitude of each coefficient $v^\alpha(k)$ has to be modulated in function of the location of the node $\alpha \in \Omega$ relative to the location of the node $k \in \Omega$. For example, if we select $v^{\alpha_1}(k)$ and $v^{\alpha_2}(k)$ in such a way that we have

$$v^{\alpha_1}(k) > v^{\alpha_2}(k) > 0$$

- then, the solution φ will be smoother in the direction (k, α_1) than in the direction (k, α_2) .

The DSI Solution

As suggested in Figure 6, the generalized global roughness criterion $R^*(\varphi)$ is a positive quadratic function of the M variables $\{\varphi(1), \dots, \varphi(\alpha), \dots, \varphi(M)\}$ and this function can be represented by a paraboloid in a $(M + 1)$ dimensional space. The solution φ of the DSI problem corresponds to the minimum of $R^*(\varphi)$ which is characterized by the following conditions of optimality:

$$\frac{\partial R^*(\varphi)}{\partial \varphi(1)} = \dots = \frac{\partial R^*(\varphi)}{\partial \varphi(\alpha)} = \dots = \frac{\partial R^*(\varphi)}{\partial \varphi(M)} = 0$$

It can be verified that this solution is achieved if, for each $\alpha \in \Omega$, the following condition, termed the “local DSI equation,” is satisfied:

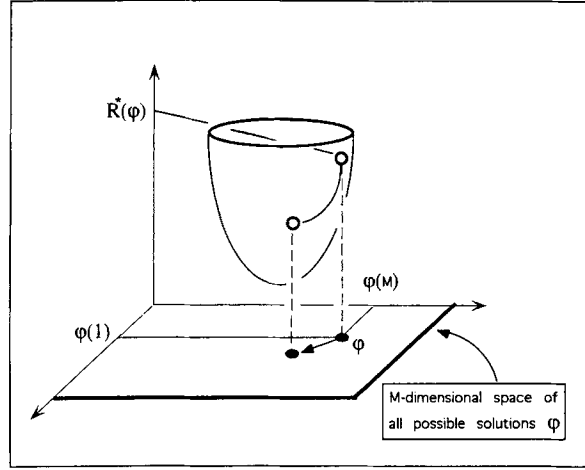


Figure 6. Generalized global roughness $R^*(\varphi)$ is quadratic function of $\{\varphi(1), \varphi(2), \dots, \varphi(M)\}$. At each iteration of DSI algorithm, function φ is updated so that this generalized global roughness is decreasing.

$$\varphi(\alpha) = \frac{\sum_{k \in N(\alpha)} \{ \mu(k) v^\alpha(k) \cdot \sum_{\substack{\beta \in N(k) \\ \beta \neq \alpha}} v^\beta(k) \cdot \varphi(\beta) \} + \sum_i \Gamma_i(\alpha)}{\sum_{k \in N(\alpha)} \mu(k) \cdot (v^\alpha(k))^2 + \sum_i \gamma_i(\alpha)}$$

with:

$$\begin{cases} \Gamma_i(\alpha) = \bar{\omega}_i \cdot A_i(\alpha) \cdot \left\{ \sum_{\beta \neq \alpha} A_i(\beta) \cdot \varphi(\beta) - b_i \right\} \\ \gamma_i(\alpha) = \bar{\omega}_i \cdot (A_i(\alpha))^2 \end{cases}$$

This local DSI equation can be written as

$$\varphi(\alpha) = -\frac{G(\alpha) + \Gamma(\alpha)}{g(\alpha) + \gamma(\alpha)}$$

where $G(\alpha)$ and $g(\alpha)$ are terms induced by the minimization of the roughness at node α whereas $\Gamma(\alpha)$ and $\gamma(\alpha)$ are terms corresponding to the minimization of the degree of violation of the constraints attached to node α :

$$\left| \begin{array}{l} G(\alpha) = \sum_{k \in N(\alpha)} \left\{ \mu(k) v^\alpha(k) \cdot \sum_{\substack{\beta \in N(k) \\ \beta \neq \alpha}} v^\beta(k) \cdot \varphi(\beta) \right\} \\ g(\alpha) = \sum_{k \in N(\alpha)} \mu(k) \cdot (v^\alpha(k))^2 \end{array} \right. \quad \text{and} \quad \left. \begin{array}{l} \Gamma(\alpha) = \sum_i \Gamma_i(\alpha) \\ \gamma(\alpha) = \sum_i \gamma_i(\alpha) \end{array} \right|$$

The local DSI equation presented here suggests to use the following iterative algorithm for determining the DSI solution φ :

```

let  $I$  be the set of nodes where  $\varphi(\alpha)$  is unknown
let  $\varphi$  be a given initial approximated solution
while (more iterations are needed)
    {
      for_all ( $\alpha \in I$ )
        {
          
$$\varphi(\alpha) = -\frac{G(\alpha) + \Gamma(\alpha)}{g(\alpha) + \gamma(\alpha)}$$

        }
    }

```

This algorithm has been proven to be convergent (Mallet, 1989a, 1992b) whatever the initial solution could be and, of course, it converges to the unique solution when the conditions ensuring the uniqueness of the DSI solution are satisfied.

Remark

In the previous section, the “local DSI equation” was presented, which is used for determining iteratively the DSI solution. It may be interesting to point out that this DSI solution φ also satisfies the following “global DSI equation” (see Mallet, 1992b):

$$[W] \cdot \varphi = Q$$

In this matrix equation, φ and Q are column vector of size $M = |\Omega|$ whereas $[W]$ is a $M \times M$ semipositive symmetric matrix:

- $[W]$ depends only:
 - on the topology of the graph $\mathcal{G}(\Omega, N)$,
 - on the given weighting coefficients $\{v^\alpha(k)\}$ and $\mu(k)$,
 - on the constraints.
- Q depends only on the constraints and is equal to the null column vector in the situation where there is no constraint.

For example, in the situation where there is no constraint, the element $W_{\alpha\beta}$ located on row α and column β of $[W]$ is such that:

$$W_{\alpha\beta} = \sum_{k \in \{N(\alpha) \cap N(\beta)\}} \mu(k) \cdot v^\alpha(k) \cdot v^\beta(k)$$

Generalization of the DSI Method

In practical applications the function φ of the discrete model $\mathfrak{M}(\Omega, N, \varphi, \mathcal{C})$ may have several components interacting through “cross constraints” and the simplified version of the DSI method presented in the previous paragraph has to be extended somewhat for taking care of the multicomponent situation where:

$$\varphi(\alpha) = \{\varphi^x(\alpha), \varphi^y(\alpha), \varphi^z(\alpha), \dots, \varphi^v(\alpha), \dots\} \quad \forall \alpha \in \Omega$$

It is possible to change slightly the notations in the definition of the local roughness criterion $R(\varphi|k)$ and the degree of violation of the constraints $\rho(\varphi|C_i)$ in such a way that the solution to the multicomponent problem can be obtained with generalized local DSI equations *formally* identical to the one obtained in the situation where φ has only one component. For that purpose, it is simply suggested to redefine $R(\varphi|k)$ and $\rho(\varphi|C_i)$ as follows:

$$R(\varphi|k) = \sum_v r^v \cdot \left| \sum_{\alpha \in N(k)} v_v^\alpha(k) \cdot \varphi^v(\alpha) \right|^2$$

$$\rho(\varphi|C_i) = \left| \sum_{\alpha \in \Omega} \sum_v A_i^v(\alpha) \cdot \varphi^v(\alpha) - b_i \right|^2$$

In the definition of the roughness $R(\varphi|k)$, r_v is a *given* positive weighting coefficient allowing to modulate the contribution of the function $\varphi^v(\cdot)$ to the local roughness $R(\varphi|k)$. If the functions $\{\varphi^v(\cdot)\}$ have approximately the same magnitude, then one, for example, can select all the coefficients $\{r_v\}$ equal to 1.

The equation allowing to update the value $\varphi^v(\alpha)$ in the iterative DSI algorithm keeps formally almost unchanged and becomes:

$$\varphi^v(\alpha) = \frac{r_v \cdot \sum_{k \in N(\alpha)} \left\{ \mu(k) v_v^\alpha(k) \cdot \sum_{\substack{\beta \in N(k) \\ \beta \neq \alpha}} v_v^\beta(k) \cdot \varphi^v(\beta) \right\} + \sum_i \Gamma_i^v(\alpha)}{r_v \cdot \sum_{k \in N(\alpha)} \mu(k) \cdot (v_v^\alpha(k))^2 + \sum_i \gamma_i^v(\alpha)}$$

with:

$$\begin{cases} \Gamma_i^v(\alpha) = \bar{\omega}_i \cdot A_i^v(\alpha) \cdot \left\{ \sum_{\beta \neq \alpha} A_i^v(\beta) \cdot \varphi^v(\beta) - b_i + c_i^v \right\} \\ \gamma_i^v(\alpha) = \bar{\omega}_i \cdot (A_i^v(\alpha))^2 \\ c_i^v = \sum_{\eta \neq v} \sum_{\beta} A_i^\eta(\beta) \cdot \varphi^\eta(\beta) \end{cases}$$

The only noticeable difference with the monocomponent situation is the introduction of the terms c_i^v which occur only in the situation of cross constraints

involving several components of φ . When there is no such cross constraint attached to the node α , then the given formulae are strictly identical to the one corresponding to the monocomponent case presented in a former paragraph.

Implementing the DSI Method

In spite of its apparent complexity, the local DSI equation is simple to program and the heart of the iterative algorithm can be implemented in about 30 lines of C++ source code. The real programming difficulty comes from the discrete model $\mathfrak{M}(\Omega, N, \varphi, \mathcal{C})$ which has to be implemented in order to:

- optimize the access to the neighborhoods $N(\alpha)$ and the values $\varphi'(\alpha)$ used by the DSI equation,
- take care of its “self-consistency” when modifications occur in Ω , $N(\cdot)$, φ or \mathcal{C} .

Implementing a totally general algorithm taking care of the two items here may result in a large software with more than 100 thousands lines of C++ source code playing the role of a server for the 30 lines corresponding to the DSI algorithm. Such an heavy machinery is not always necessary and its description is beyond the scope of this paper.

In order to have an idea of the nature of the problems, let us glance at Figure 7. This figure represents a triangulated surface and a set of data points

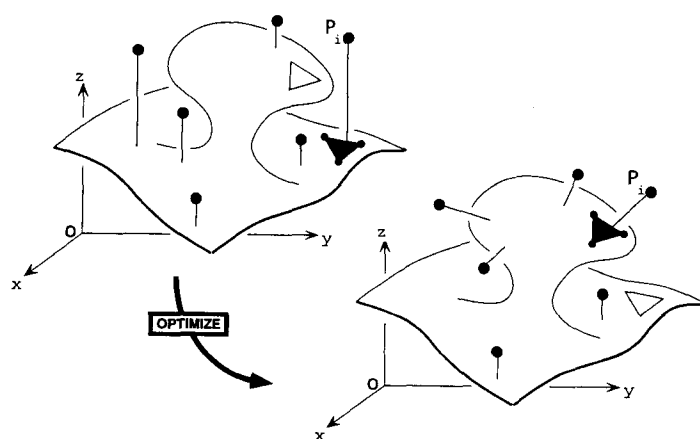


Figure 7. Each point P_i is assumed to hold data $\phi(P_i)$ which are projected on triangulated surface in direction $\Delta(P_i)$ specific to P_i . Data $\phi(P_i)$ are transformed into constraints affecting nodes corresponding to vertices of triangle hit by $\Delta(P_i)$. If direction $\Delta(P_i)$ is changed, then different triangle is hit and constraints have to be updated.

$\{P_1, P_2, \dots\}$ where each point P_i is assumed to hold data $\phi(P_i)$ which are projected on the triangulated surface in a direction $\Delta(P_i)$ specific to P_i . The data $\phi(P_i)$ are transformed into constraints affecting the nodes corresponding to the vertices of the triangle hit by $\Delta(P_i)$. It results from this situation that:

- If the direction $\Delta(P_i)$ is changed, then a different triangle is hit and the constraints $C_i \in \mathcal{C}$ have to be updated.
- If the density of the nodes in a region of the model is changed in order to get a better numerical approximation then, the set Ω and the neighborhoods $\{N(\alpha): \alpha \in \Omega\}$ are changed and it is necessary to update constraints $C_i \in \mathcal{C}$ in order to take care of these modifications.

EXAMPLES

The field of application of the notions of Discrete Model and Discrete Smooth Interpolation presented in this paper is large and the selection of a specific example is difficult. It is proposed in Figures 8 and 9 two discrete models corresponding, respectively, to the modeling of the geometry of a salt dome and to the modeling of a seismic velocity field in a regular rectilinear 3D grid:

- The first example presented in Figure 8 corresponds to the modeling of the geometry of a salt dome. In Figure 8A, you can see about 100 data points P_i which are assumed to be located on the surface to build. As suggested in Figure 7, each of these data points is projected on the surface according to a specific direction $\Delta(P_i)$ hitting a triangle $T_i(\alpha_0, \alpha_1, \alpha_2)$ at a point P_i^* . It is possible to define a linear constraint C_i on

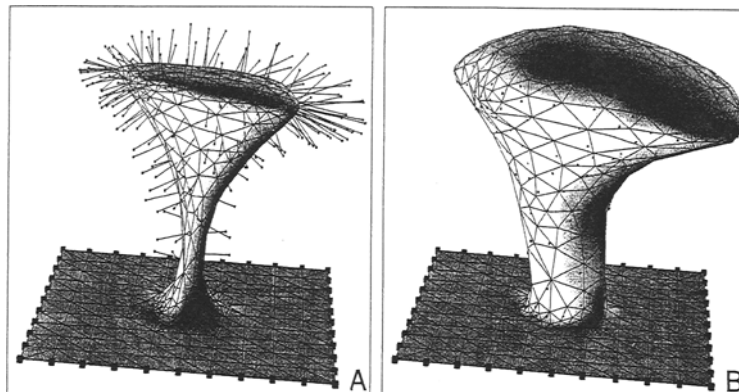


Figure 8. Modeling salt dome with DSI: A, initial model and data; and B, final model.

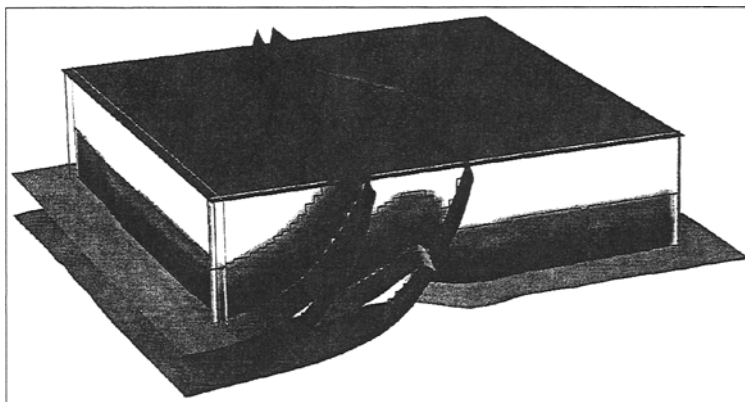


Figure 9. Modeling seismic velocities in parallelepipedic volume of subsurface. Volume is filled by rectilinear 3D grid cut by geological horizons and faults. Variations of velocity stored in grid are displayed in shaded mode.

the nodes $(\alpha_0, \alpha_1, \alpha_2)$ specifying that P_i should be coincident with P_i^* . The modeling process is decomposed into three steps:

- (1) In a first step, an initial discrete model $\mathfrak{M}(\Omega, N, \varphi, \mathcal{C})$ consisting of a rectangular triangulated surface is created in the neighborhood of the data points $\{P_i\}$.
- (2) Each data point P_i is projected on the closest point of this initial surface and is transformed into a constraint $C_i \in \mathcal{C}$ constraining the components $(\varphi^x, \varphi^y, \varphi^z)$ corresponding to the location of the nodes of the surface.
- (3) The DSI algorithm is applied and, after convergence, if necessary, for giving more flexibility to the surface, the triangles can be split where the distance $d(P_i, P_i^*)$ is bigger than a given threshold and return to the item (2). Moreover, as suggested in Figure 7, between two iterations of the DSI algorithm, it also is possible to optimize the directions of projection $\Delta(P_i)$.

After some iterations of this process, we get the model represented in Figure 8B.

- The second example presented in Figure 9 corresponds to the modeling of a seismic velocity in a parallelepipedic volume of the subsurface. This volume is filled by a regular rectilinear 3D grid having 200 steps in the x -direction, 200 steps in the x -direction, and 100 steps in the z -direction. This grid is assumed to be cut by some horizons and listric faults and the velocities $\phi^v(P_i)$ are known at 150 points $\{P_i\}$ irregularly distributed

in the volume. Each data point $\{P_i, \phi^v(P_i)\}$ is transformed into a constraint specifying that the velocity $\phi^v(\alpha_0)$ of the closest node α_0 should be equal to the given value $\phi^v(P_i)$. The variations of the velocities, restricted to one layer, are displayed in shaded mode on the faces of the parallelepipedic volume represented in Figure 9. As can be seen, all the discontinuities corresponding to the intersections of the grid with the horizons and faults have been strictly taken into account. However, it should be noticed that, if necessary, we could maintain some partial continuity across these surfaces if we keep randomly some few connections between nodes located on both sides of these surfaces; in this situation, the density of the connections to be kept could be modeled as a property of the surfaces.

In both of these two examples, for the DSI method, the coefficients $\{v^\alpha(k)$ the ‘‘harmonic weights’’ presented in a previous paragraph are used and the stiffness function $\mu(k)$ was selected constant equal to 1. The number of iterations was taken equal to 10.

CONCLUSIONS

In practice, the DSI method has proven to be an efficient numerical method and the main reasons for this success are the following:

- It is possible to implement this method in such way that the same software can interpolate the geometry and the properties of curves, surfaces, and solids. This surprising flexibility is the result of the fact that the DSI method does not need to know the dimension of the graph $\mathcal{G}(\Omega, N)$. It is even possible to apply DSI to discrete models having a nonuniform dimension and which are locally isomorph to a curve, a surface, or a solid. For example this is the situation of a ‘‘high permeability region’’ in a 3D layer which is locally a microchannel (= a curve) connected to a permeable fault (= a surface) itself intersecting a permeable lens (= a solid).
- It is potentially possible to account for any type of data provided that these data can be turned into linear constraints.
- In the parts of an object $\mathfrak{M}(\Omega, N, \varphi, \mathcal{C})$ where the constraints $C_i \in \mathcal{C}$ are contradictory, these constraints behave in a least-square sense and the associated certainty factors $\tilde{\omega}_i^2$ control their behavior. For example if a part of a surface is attracted by two data points P_1 and P_2 located on two sides of this surface, then the surface will pass in between the points P_1 and P_2 and will be closer to P_1 if the certainty factors of P_1 is greater than the one of P_2 .

- In the parts of an objects $\mathfrak{M}(\Omega, N, \varphi, \mathcal{C})$ where the constraints $C_i \in \mathcal{C}$ are consistants, these constraints are respected almost perfectly and behave as if they where “hard” constraints. This is surprising when we remember that, from a mathematical point of view, the constraints are taken into account in a least-square sense.
- It is extremely easy to account for discontinuity: we have only to build the topological model $\mathcal{G}(\Omega, N)$ in such a way that it respects these discontinuities.
- It also is easy to account for anisotropies. This can be achieved in two different ways: either by defining the weighting coefficients $\{v^\alpha(k)\}$ in such a way that they integrate this anisotropy or by introducing some special constraints modeling this anisotropy. It is important to notice that the anisotropy can be heterogeneous and can change from one node $\alpha \in \Omega$ to another.
- The iterative algorithm converges fast and even for models having several thousands of nodes, the solution can be obtained in real time on most of the current workstations. Moreover, the more we have constraints, the more the method converges rapidly; at the limit, if there is enough consistant constraints, the method may converge in 1 iteration.
- The last but not the least, the DSI method is numerically stable, even if the data are clustered.

From a theoretical part of view, the most interesting aspect of DSI mentioned is certainly the fact that this generic interpolation method is decoupled completely from the data: the only thing that this method can see are constraints induced by the data and not the data themselves. Thus, an existing software does not have to be changed each time a new type of data is introduced in the modeling process. This is promising for the future and I hope that many geomathematicians will propose new types of DSI constraints.

ACKNOWLEDGMENTS

The research presented in this paper has been performed in the frame of the GOCAD project, and I would like to thank all the current sponsors of this project for their active support. I also would like to thank the anonymous reviewer who gave me some important references related to discrete modeling.

REFERENCES

- Akima, H., 1978, A method for bivariate interpolation and smooth surface fitting for irregularly distributed data points: ACM Trans. on Mathematical Software, v. 4, no. 2, p. 148–159.
- Arthur, D. W. G., 1965, Interpolation of a function of many variables: Photogrammetric Engineering and Remote Sensing, v. 31, no. 2, p. 348–349.

- Aziz, K., and Settari, A., 1979, Petroleum reservoir simulation: Elsevier, New York, 476 p.
- Bass, J., 1971, Cours de mathematiques, tome 3: topologie, integration, distributions, equations integrales, analyse harmonique (in French): Masson et Cie, Paris, 389 p.
- Bergthorsson, P., and Doos, B. R., 1955, Numerical weather map analysis: *Tellus VII*, v. 3, no. 1, p. 329-340.
- Bezier, P., 1974, Mathematical and practical possibilities of UNISURF: Academic Press, New York; *Computer Aided Geometric Design*, v. 1, no. 1, p. 19-35.
- Briggs, I. C., 1974, Machine contouring using minimal curvature: *Geophysics*, v. 39, no. 1, p. 39-48.
- de Boor, C., 1978, A practical guide to splines: Applied Mathematical Sciences No. 27, Springer Verlag, Berlin, 245 p.
- Farin, G., 1988, Curves and surface for computer aided geometric design, a practical guide: Academic Press, San Diego, 334 p.
- Gill, P. E., Murray, W., and Wright, M. H. 1981, Practical optimization: Academic Press, San Diego, 401 p.
- Harder, R. L., and Desmarais, R. N., 1972, Interpolation using surface splines: *Jour. Aircraft*, v. 9, no. 2, p. 189-191.
- Horton, R. E., 1923, Rainfall interpolation: *Mon. Wea. Rev.*, v. 51, no. 6, p. 291-304.
- Mallet, J. L., 1989a, Procédé de codage et d'ajustement de surfaces complexes: French Patent No. 89-12341, 45 p.
- Mallet, J. L., 1989b, Discrete smooth interpolation: *ACM-Transactions on Graphics*, v. 8, no. 2, p. 121-144.
- Mallet, J. L., 1992a, gOcad: A Computer Aided Design program for geological applications, in Turner, K., ed., Three-dimensional modelling with geoscientific information systems: Nato ASI Series C, v. 354, Kluwer Acad. Publ. Dordrecht, The Netherlands, p. 123-141.
- Mallet, J. L., 1992b, Discrete Smooth Interpolation in geometric modelling: *Computer Aided Design*, v. 24, no. 4, p. 178-191.
- Mortenson, F., 1985, Geometric modelling: John Wiley & Sons, New York, 763 p.
- Overveld, C. W., 1995, Pondering on discrete smoothing and interpolation: *Computer Aided Design*, v. 27, no. 5, p. 377-384.
- Sibson, R., 1981, A brief description of natural neighbour interpolation, in Barnett, V. ed., *Interpolating multivariate data*: John Wiley & Sons, New York, p. 21-36.
- Weaver, R. C., 1964, Relative merits of interpolation and approximating functions in the grade prediction problem, in Parks, G. A., ed., *Computers in the mineral industries, Part 1*: Stanford Univ. Publ., Geological Sciences, v. 9, no. 1, p. 171-185.
- Whittaker, E. T., 1923, On a new method of graduation: *Proc. Edinburgh Math. Soc.*, v. 41, no. 1, p. 63-75.